Proceedings of the 21st International Conference on Low Temperature Physics
Prague, August 8-14, 1996

Part S6 - Plenary and invited papers

Phase Diagram of $Bi_2Sr_2CaCu_2O_8$ in the mixed state: effects of anisotropy and disorder

B. Khaykovich[1], E. Zeldov[1], M. Konczykowski[2], R. A. Doyle[1,3], D. Majer[1], P. H. Kes[4], and T. W. Li[4]

[1]Department of Condensed Matter Physics, The Weizmann Institute of Science, 76100 Rehovot, Israel

[2]CNRS, URA 1380, Laboratoire des Solides Irradiés, École Polytechnique, 91128 Palaiseau, France

[3]IRC in Superconductivity, University of Cambridge, Cambridge CB3 0HE, United Kingdom

[4]Kamerlingh Onnes Laboratorium, Rijksuniversiteit Leiden, P. O. Box 9506, 2300 RA Leiden, The Netherlands

The vortex-lattice phase transitions in $Bi_2Sr_2CaCu_2O_8$ crystals with various oxygen stoichiometry and artificially induced disorder are studied using local magnetization measurements. The first-order phase transition line at elevated temperatures shifts upward for more isotropic over-doped samples. At lower temperatures another sharp transition is observed at the onset of second magnetization peak. The two lines merge at a multicritical point at intermediate temperatures forming apparently a continuous phase transition line that is anisotropy dependent. Weak point disorder preserves the first-order transition and shifts it to lower fields. This shift is accompanied by a corresponding downward shift of the second magnetization peak. A low density of columnar defects shifts the first-order transition to higher fields, apparently transforming it into a continuous transition. The first-order transition in clean crystals is concluded to involve melting of the vortex-lattice. Schematic phase diagram based on this study is presented.

1. INTRODUCTION

The high-temperature superconductors (HTSC) in the mixed state display a very complicated phase diagram. The nature of the different vortex phases and the transitions between them are still unclear. The recent discovery of a first-order vortex-lattice phase transition (FOT) is of significant fundamental and practical interest and may help to resolve some of the open questions [1-13]. In magnetic measurements this transition manifests itself as a sharp step in magnetization vs. temperature or applied field [10] at high temperatures. In $Bi_2Sr_2CaCu_2O_8$ (BSCCO) crystals the sharp step disappeares suddenly at some critical point T_{cp}. At lower temperature there is a sharp onset of bulk critical current at the anomaluos second magnetization peak, which is probably due to second-order phase transition of the vortex-lattice [13]. We have investigated the effect of anisotropy on the two phase transitions. It is generally accepted that high anisotropy plays a crucial role in the richness of the phase diagram of high-temperature superconductors. For the different anisotropy crystals the two phase transition lines are found to form apparently one continuous transition line that changes from first to possibly second order at a critical point. This line is anisotropy dependent and shifts to higher fields for more isotropic crystals.

We also study how the different vortex phases and the transitions between them are changed with enhanced disorder in the crystal structure of BSCCO. The FOT is expected to occur only in very clean systems, whereas in the presence of strong disorder only continuous phase transitions or crossovers are anticipated [1, 14]. Artificially induced disorder may therefore have a profound effect on the mixed state phase diagram, substantially modifying the structure, dimensionality, and pinning behavior of the various vortex phases, and shifting the boundaries between the phases [1]. Until now most of the experimental and theoretical efforts have focused on the rather extreme cases of clean [1-12] and highly disordered systems [1, 14, 15, 16], respectively. In contrast, the general knowledge of the effects of *weak* disorder on the first-order transition is very limited.

In addition to the fundamental interest in the effect of incorporation of weak disorder, we use this

approach as a weakly perturbative tool to probe the underlying physics governing the FOT. In particular, the three prevailing theoretical descriptions of the FOT can be classified as melting, evaporation, or sublimation [1]. The more commonly accepted scenario is melting of an ordered *solid* flux-line lattice into a vortex-line *liquid* [2, 3]. In the evaporation (decoupling) transition the vortex-line *liquid* dissociates into a *gas* of uncorrelated vortex pancakes in the individual CuO planes [4]. Recently a sublimation transition (simultaneous melting and decoupling) was proposed in which the *solid* line-lattice undergoes a direct transition into the pancake *gas* [5]. The equilibrium magnetization measurements in clean BSCCO crystals [10] do not reveal which of the specific mechanisms is the origin of the observed FOT.

We investigate the vortex-lattice phase transitions in BSCCO crystals in the presence of either weak point disorder or a low density of correlated disorder. We show that these two types of defects have very distinctive and different effects. Weak point disorder preserves the FOT and shifts it to lower fields together with a shift of the anomalous second magnetization peak. Columnar defects significantly enhance vortex pinning below the transition and shift the transition line to higher fields. We find that the vortex phase below the transition has a finite shear modulus and hence conclude that the observed FOT is either melting or sublimation of a solid vortex-lattice, rather than evaporation of a vortex liquid.

2. EXPERIMENTAL

The experiments were carried out on several as-grown BSCCO crystals [17, 18] with typical dimensions of 700 × 300 × 10 μm^3 and on two crystals [18] which were heat treated in order to change the oxygen stoichiometry [19]. The as-grown crystals [17, 18] show practically identical phase diagrams. The over-doped crystal (annealed at 500°C in air) has $T_c \simeq 83.5$ K and the optimally-doped crystal (annealed at 800°C) has $T_c \simeq 89$ K. As shown in [19] annealing in air between 500°C and 800°C reversibly changes the oxygen stoichiometry. With increasing oxygen content both the c-axis and T_c decrease linearly with the oxygen concentration. It was convincingly shown [13] that also the anisotropy in BSCCO depends on oxygen contents and the crystal becomes more isotropic in going from optimally to over-doped. The as-grown crystals [17, 18] have doping level close to optimal ($T_c \simeq 90$ K), but the exact oxygen stoichiometry is not known due to the large

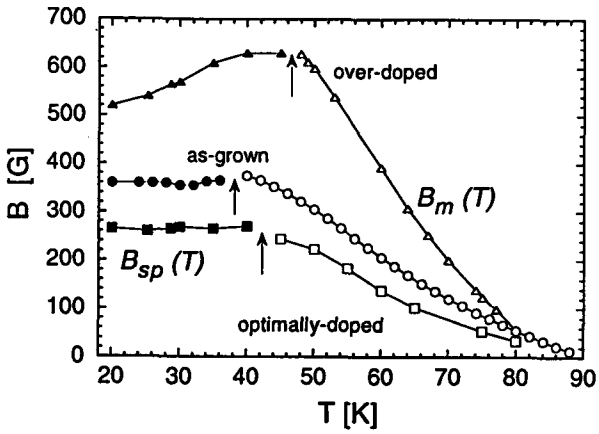

Figure 1: First-order transition lines $B_m(T)$ (empty symbols) together with the second-order transition $B_{sp}(T)$ (filled symbols) for over-doped sample with $T_c \simeq 83.5$ K (△), as-grown sample $T_c \simeq 90$ K (○), and optimally-doped BSCCO crystal with $T_c \simeq 89$ K (□). $B_{sp}(T)$ was defined as the point of the steepest drop of the local magnetization peak on decreasing field. The arrows indicate the position of the critical point.

vertical temperature gradient during the growth and *in situ* annealing process [18].

For study of disorder effects as-grown BSCCO crystals were irradiated by 2.5 MeV electrons, 1 GeV Xe ions, or 0.9 GeV Pb ions. Electron irradiation at two different doses, 3×10^{18} cm^{-2} and 6×10^{18} cm^{-2}, was performed at École Polytechnique (France) at low temperatures (20 K). Heavy-ion irradiation was performed at GANIL (Caen, France). Electron irradiation at low temperatures is known to produce point defects on all sublattices (Frenkel pairs), however on warming the sample to room temperature some clustering occurs due to defect migration and recombination [20]. The resulting damage is in the form of a random spread of point defects and small clusters with size below the resolution of electron microscopy. The total damage can be expressed in units of displacement per atom (dpa) and is estimated to be of the order of 5×10^{-4} and 10^{-3} dpa for our two irradiation doses [20]. In contrast, swift heavy ions produced columnar defects extending through the crystal thickness parallel to the crystalline c-axis [21]. In this study we have investigated very low irradiation doses corresponding to matching fields B_ϕ of 20, 50, and 100 G ($B_\phi = n\phi_0$, where n is the den-

sity of the columnar tracks and ϕ_0 is the magnetic flux quantum). The local magnetization measurements were performed in applied field $H_a||z||$c-axis using arrays of $10 \times 10\mu m^2$ GaAs/AlGaAs Hall sensors [22].

3. EFFECTS OF ANISOTROPY

Figure 1 shows the mapping of the first-order transition as a function of temperature for three crystals of different oxygen stoichiometry, i.e. different anisotropy. We find that the transition line shifts significantly with anisotropy and moves to higher fields for more isotropic crystals. In addition, in all the crystals the first-order transition terminates abruptly at a sample dependent critical point (indicated by arrows) in the range of 40 to 50 K [10]. Figure 1 also shows the second peak line $B_{sp}(T)$ for three crystals along with $B_m(T)$. The position of B_{sp} is strongly anisotropy dependent [23]. We find that it shifts to higher fields to the same extent as the shift of $B_m(T)$. Moreover, the first-order transition terminates at a temperature below which the second magnetization peak develops for each of the samples [13, 22-26]. $B_{sp}(T)$ and $B_m(T)$ merge at two sides of the same, sample dependent, critical point on the $B-T$ phase diagram for the various anisotropies. This finding is a strong indication that the two lines represent in fact one continuous vortex-lattice transition that changes from a first-order to probably a second-order (or a weakly first-order) at a tricritical point as the temperature is decreased. This interpretation is consistent with the fact that a first-order vortex-lattice phase transition is not expected to terminate at a simple critical point and should be followed by a second-order phase transition due to involved symmetry breaking. In fact we beleive that the FOT splits into two second-order phase transitions at the critical point as discussed below. The amplitude of the second magnetization peak decreases as the temperature is increased, and the peak becomes not very well-defined close to the critical point probably due to rapid relaxation of the bulk current at higher temperatures. This is the reason for the apparent gap in the data in a narrow temperature interval around the critical point (Fig. 1).

4. EFFECTS OF POINT DISORDER

Figure 2 illustrates the FOT step in the equilibrium magnetization at 86K of an unirradiated BSCCO crystal [17] along with another crystal from the same batch but irradiated with doses of 3×10^{18}

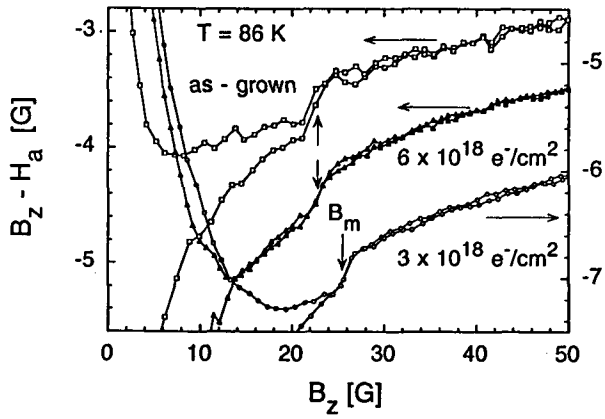

Figure 2: Local magnetization loops $B_z - H_a$ vs. B_z ($T = 86$ K) measured on BSCCO crystals [17] before (□) and after 2.5 MeV electron irradiation of 3×10^{18} cm^{-2} (○) and 6×10^{18} cm^{-2} (△).

cm^{-2} and 6×10^{18} cm^{-2} electrons. The first-order transition is clearly preserved after electron irradiation. This is in contrast to $YBa_2Cu_3O_7$ crystals where comparable irradiation doses were shown to completely suppress the resistively measured FOT [27]. At lower temperatures the magnetization step in BSCCO is slightly smeared after irradiation, which is consistent with the theoretical prediction of some rounding of the FOT in weakly disordered systems [28]. However we find that the first-order transition is still clearly preserved. Figures 3a and 3b show the FOT line, $B_m(T)$, of crystals irradiated with electrons to various doses compared with as-grown crystals. The FOT line is found to shift to *lower* fields with electron irradiation. This shift is negligible at high temperatures, increases gradually with decreasing temperature, and becomes most pronounced close to the critical point T_{cp} [10], where the FOT lines show unexpected flattening and then terminate. The second-order vortex-glass transition is predicted to shift to higher fields with increased disorder [1]. On the other hand, there is currently no theoretical consensus regarding the expected direction of the shift (if any) of the first-order transition [29, 30, 31]. Our findings show that weak point disorder shifts the FOT to *lower* fields in contrast to the glass transitions [1, 30]. The effect of disorder grows as one moves along the FOT line to lower temperatures as theoretically proposed [31, 32]. Further, we observe no substantial increase in pinning with electron irradiation and the hysteretic magnetization behaviour at elevated temperatures is still governed

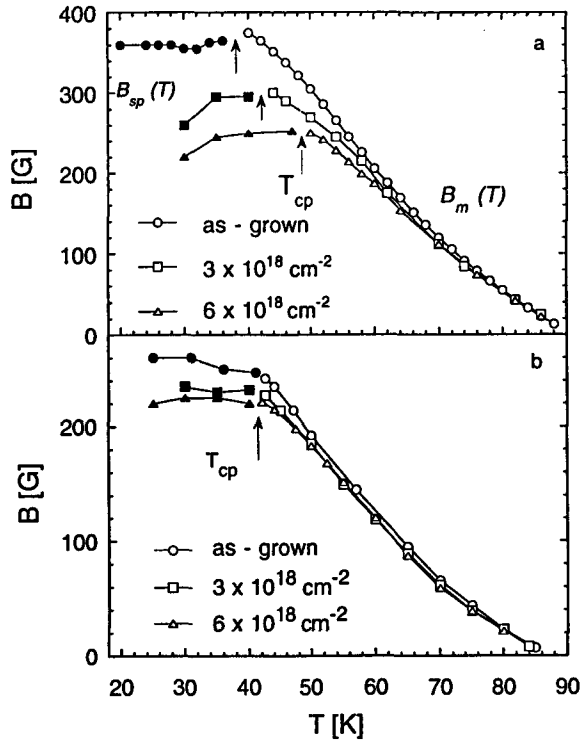

Figure 3: Mapping of the first-order transition lines $B_m(T)$ (empty symbols) together with the second-order transition $B_{sp}(T)$ (filled symbols) for BSCCO crystals [17] (a) and [18] (b) for different doses of 2.5 MeV electron irradiation.

by surface and geometrical barriers [33] rather than by bulk pinning. It is interesting, however, that the weak disorder, which has no appreciable effect on pinning, has a significant effect on the position of the FOT line.

At temperatures below T_{cp} a sharp second magnetization peak is observed at $B_{sp}(T)$. It has been suggested [8, 13, 24] that this peak is triggered by an underlying phase transition of a weakly pinned ordered vortex-lattice into a highly disordered, possibly decoupled or entangled, vortex solid [4, 31, 32]. Figure 3 shows that $B_{sp}(T)$ shifts downward with point disorder [34] in agreement with recent theoretical suggestions [32], indicating that the state above $B_{sp}(T)$ is indeed a highly disordered vortex phase. In all samples, $B_{sp}(T)$ and $B_m(T)$ merge at the critical point, forming a continuous line that shifts to lower fields with increased disorder. Our findings here demonstrate that the phase transition line is sensitive to *both* the disorder and anisotropy. However the individual effects are quite distinctive and may be separated. The penetration depth and anisotropy determine the slope of $B_m(T)$ near T_c and correspondingly shift the entire line [13, 24] as shown in Fig. 1. The as grown sample [17] in Fig. 3a for example is more isotropic than that in Fig. 3b [18], with about twice as large a slope of $B_m(T)$ at high temperatures. Disorder on the other hand has practically no effect at higher temperatures and mainly governs the 'flattening' of the $B_m(T)$ at lower temperatures and its crossover into $B_{sp}(T)$. This finding strongly suggests that even in the as-grown crystals the second peak transition, the critical point, and the flattening of $B_m(T)$ are driven by the intrinsic disorder of the crystals. Thus the question of the existence of the second peak transition in the limit of vanishing disorder is an open one and of considerable interest [31, 32]. It is also interesting to note that the $B_{sp}(T)$ line often shows a tendency to decrease with decreasing temperature [13]. Since we find that point disorder shifts this line down, this unexplained behavior could now be understood in view of the increasing role of disorder with decreasing temperature.

5. EFFECTS OF CORRELETED DISORDER

Next we turn to the analysis of correlated disorder. Columnar defects apparently have a profoundly different effect on the melting transition when compared to point disorder. Figure 4 shows the local magnetization loop of an unirradiated BSCCO crystal [17] in the vicinity of the FOT at 60K along with a crystal irradiated with 1 GeV Xe ions at a very low dose of B_ϕ = 20 G (the average distance between tracks is about 1μm). The unirradiated crystal shows practically reversible magnetization below $B_m(T)$. A small density of columnar defects causes the appearance of very pronounced hysteresis even for $B \gg B_\phi$. Analysis of field gradient $dB_z(x)/dx$ loops following the procedure of Ref. [33] confirms that the observed hysteresis is caused by bulk vortex pinning and not by surface effects. The effectiveness of the pinning by this low dose of columnar defects when compared to point defects, is even more striking considering that our electron irradiation results in the displacement of about 10^{-3} atoms as compared to only about 3×10^{-5} atoms by columnar de-

fects. This strong bulk pinning terminates abruptly at the bulk irreversibility field $B_{IB}(T)$ which is located at the original FOT line $B_m(T)$ as shown in Fig. 5 (compare $B_m(T)$ line with $B_{IB}(T)$ line for $B_\phi = 20$ G). In fact at high temperatures we can still resolve the FOT magnetization step as shown at $T = 85$ K in the inset of Fig. 5. So very low doses of columnar defects pin the vortex-lattice below the transition while preserving the first-order nature of the phase transition at high temperatures and low fields. At lower temperatures like in Fig. 4 the step is not resolved, either due to possible masking by the strong pinning or due to the transformation of the FOT into a second-order transition [30].

The above findings are strong evidence that the observed FOT is either melting or sublimation, rather than an evaporation transition. In Fig. 4 for example, the magnetic field at melting is about $B_m(T) \simeq 200$ G, an order of magnitude larger than $B_\phi = 20$ G. Thus just one columnar defect per ten vortices results in substantial pinning below the transition, indicating a finite shear modulus and hence a *solid* vortex phase below the FOT. These finding are consistent with recent resistive measurements of BSCCO crystals at low fields [9]. At higher irradiation doses, $B_\phi = 50$ G and 100 G, the bulk pinning still terminates abruptly, but the corresponding $B_{IB}(T)$ is now significantly shifted toward higher fields as shown in Fig. 5. This effect of the columnar defects is in sharp contrast to the effect of point disorder which results in a shift of the transition line to lower fields. Further, weak point disorder preserves the first-order nature of the transition whereas the higher doses of the columnar defects seem to transform it into a continuous transition since no step in magnetization could be resolved.

The bulk irreversibility line $B_{IB}(T)$ at $B_\phi = 50$ G displays a very interesting phenomenon. Figure 5 shows that at low fields $B_{IB}(T) \simeq B_m(T)$, at higher fields B_{IB} rises significantly and reaches a maximum relative deviation in the range of 100 to 150 G, and then decreases again approaching the original $B_m(T)$ line at higher fields. This remarkable behavior can be interpreted as follows. At fields comparable to B_ϕ each vortex is effectively pinned by a columnar defect and the pinning interaction outweighs the vortex-vortex interactions. As a result, the pinned vortex lattice remains intact at the original $B_m(T)$ and the melting occurs only at higher temperatures. This effect should be most pronounced at fields comparable to B_ϕ. At fields significantly higher than B_ϕ only a small fraction of vortices is pinned by the columns

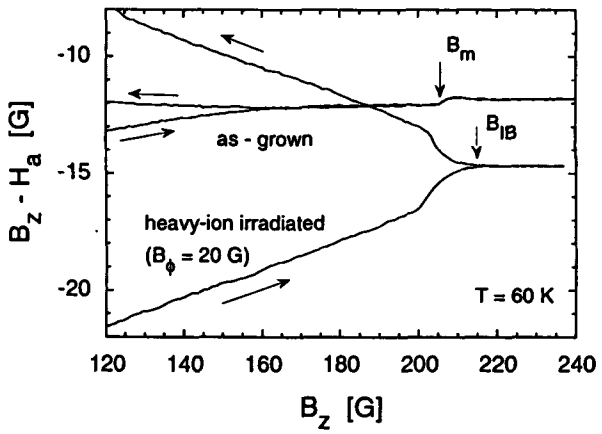

Figure 4: Local magnetization loops $B_z - H_a$ vs. B_z ($T = 60$ K) of BSCCO crystals before and after heavy-ion irradiation (1 GeV Xe) with low dose of $B_\phi = 20$ G. The onset of bulk pinning $B_{IB}(T)$ for irradiated sample and the FOT step for the as-grown crystal are indicated by arrows.

and hence the pinning of the entire lattice becomes inefficient above $B_m(T)$. As a result $B_{IB}(T)$ for $B_\phi = 50$ G approaches $B_m(T)$ at higher fields (see Fig. 5). The FOT in unirradiated crystals is observed only up to fields of about 350 G. Thus $B_\phi = 100$ G is large enough to result in a substantial shift of the transition over almost the entire field range. At very low fields, on the other hand, the original $B_m(T)$ probably occurs above the depinning temperature of columnar defects so that vortex-vortex interactions are dominant and hence no significant shift of the transition occurs (see Fig. 5). The effects of columnar defects in the regime discussed above were recently analyzed theoretically within the Bose-glass description [30]. The Bose-glass transition $B_{BG}(T)$ in irradiated samples is predicted to occur above $B_m(T)$ with a largest shift at fields comparable to B_ϕ and small effects at high and low fields, in very good qualitative agreement with the data in Fig. 5. It is thus very tempting to interpret our $B_{IB}(T)$ as the Bose-glass transition.

Figure 5 also shows the second peak transition $B_{sp}(T)$ at lower temperatures. For $B_\phi = 20$ G we can still resolve the second magnetization peak at the same field as before irradiation. At higher matching fields no peak is observed. This behavior is further significant evidence that the phase above $B_{sp}(T)$ is a highly disordered vortex solid. In this case we ex-

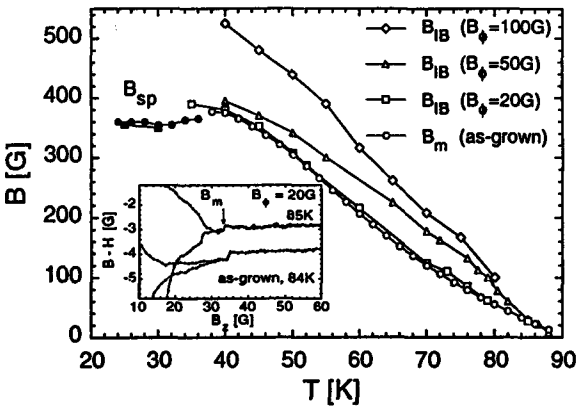

Figure 5: Mapping of the bulk irreversibility line $B_{IB}(T)$ for BSCCO crystals [17] after heavy-ion irradiation with various doses (empty symbols). The FOT line for as-grown crystal is shown for reference. The second magnetization peak lines for as-grown (filled circles) and $B_\phi = 20$ G irradiated crystal (filled squares) are shown. Inset: the magnetization step at B_m in as-grown crystal (84 K) and $B_\phi = 20$ G irradiated crystal (85 K).

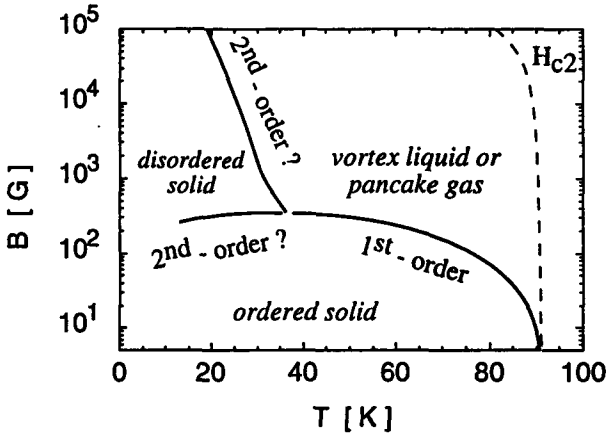

Figure 6: Schematic phase diagram of BSCCO in the mixed state. Solid lines show the phase transitions of the vortex-lattice. The critical point T_{cp} is where the FOT line splits into two possibly second-order transitions. The line separating disordered solid from the liquid phase is taken from Ref. [33]. The upper critical field H_{c2} is shown for reference by the dashed line.

pect point disorder to stabilize the high field phase and expand it on account of the ordered lattice as described above. Columnar defects are topologically similar to the ordered line-lattice and are therefore expected to have the opposite effect of stabilizing the low field phase. At $B_\phi = 20$ G only a small fraction of vortices are affected by the columns at $B_{sp} \simeq 350$ G and hence the second peak is still obtained. Higher densities of columns pin the low-field vortex-lattice very efficiently. As a result the critical current below B_{sp} becomes larger than in the disordered solid and hence the peak structure in magnetization disappears.

6. PHASE DIAGRAM

Figure 6 shows a schematic phase diagram of BSCCO. We resolve three major phases of the vortex matter separated by three phase transition lines. At low fields a rather ordered vortex-lattice is present [8]. At elevated temperatures the vortex-lattice undergoes a *strong* first-order transition with latent heat in excess of 1 k_BT per pancake vortex [10, 35]. We find strong evidence that the observed first-order transition in BSCCO crystals is either melting or sublimation of a *solid* vortex-lattice. The position of the FOT is significantly shifted to higher fields as the anisotropy of the crystals is reduced. The FOT persists in the presence of sufficiently low doses of either point-like or correlated disorder. Our results indicate that the ordered vortex-lattice transforms into a highly disordered phase at fields above the second magnetization peak [8, 32]. Weak point-disorder *destabilizes* the ordered vortex-lattice phase with respect to both the vortex-liquid and the disordered vortex-solid. Columnar defects *stabilize* the solid phase with respect to the vortex liquid and shift the transition to higher fields.

7. ACKNOWLEDGMENTS

Helpful discussions with V. M. Vinokur, V. B. Geshkenbein, L. B. Ioffe, D. R. Nelson, M. V. Feigel'man, and G. Blatter are gratefully acknowledged. We are grateful to H. Motohira for providing the as-grown BSCCO crystals and to H. Shtrikman for growing the GaAs heterostructures. This work was supported by the Ministry of Science and the Arts, Israel, and the French Ministry of Research and Technology (AFIRST), by Minerva Foundation,

Munich/Germany, by the US - Israel Binational Science Foundation, by contract CT1*CT93-0063 from the Commission of the European Union, and by the Dutch Foundation for Fundamental Research on Matter (FOM).

REFERENCES

[1] G. Blatter *et al.*, Rev. Mod. Phys. **66**, 1125 (1994); E. H. Brandt, Rep. Prog. Phys. **58**, 1465 (1995)

[2] D. R. Nelson, Phys. Rev. Lett. **60**, 1973 (1988); Nature **375**, 356 (1995).

[3] A. Houghton, R. A. Pelcovits, and A. Sudbo, Phys. Rev. B **40**, 6773 (1989); E. H. Brandt, Phys. Rev. Lett. **63**, 1106 (1989); S. Hikami, A. Fujita, and A. I. Larkin, Phys. Rev. B **44**, 10400 (1991); G. Blatter and B. I. Ivlev, Phys. Rev. B **50**, 10272 (1994); R. Sasik and D. Stroud, Phys. Rev. Lett. **75**, 2582 (1995).

[4] L. Glazman and A. Koshelev, Phys. Rev. B **43**, 2835 (1991); L. L. Daemen, L. N. Bulaevskii, N. P. Maley, and J. Y. Coulter, Phys. Rev. Lett. **70**, 1167 (1993); Phys. Rev. B**47**, 11291 (1993).

[5] G. Blatter, V. Geshkenbein, A. Larkin, and H. Nordborg, Phys. Rev. B **54**, 72 (1996).

[6] H. Safar *et al.*, Phys. Rev. Lett. **69**, 824 (1992); *ibid* **70**, 3800 (1993); W. K. Kwok *et al.*, Phys. Rev. Lett. **69**, 3370 (1992); *ibid.* **72**, 1092 (1994).

[7] H. Pastoriza *et al.*, Phys. Rev. Lett. **72**, 2951 (1994).

[8] R. Cubitt *et al.*, Nature **365**, 407 (1993); S. L. Lee *et al.*, Phys. Rev. Lett. **71**, 3862 (1993).

[9] H. Pastoriza and P.H. Kes, Phys. Rev. Lett. **75**, 3525 (1995); D. T. Fuchs *et al.*, Phys. Rev. B **54**, 796 (1996); S. Watauchi *et al.*, Physica C **259**, 373 (1996).

[10] E. Zeldov *et al.*, Nature **375**, 373 (1995).

[11] R. Liang, D. A. Bonn, and W. N. Hardy, Phys. Rev. Lett. **76**, 835 (1996); U. Welp *et al.*, (preprint).

[12] R. A. Doyle *et al.*, Phys. Rev. Lett. **75**, 4520 (1995).

[13] B. Khaykovich *et al.*, Phys. Rev. Lett. **76**, 2555 (1996).

[14] D. S. Fisher, M. P. A. Fisher, and D. A. Huse, Phys. Rev. B **43**, 130 (1991).

[15] M. V. Feigel'man, V. B. Geshkenbein, A. I. Larkin, and V. V. Vinokur, Phys. Rev. Lett. **63**, 2303 (1989).

[16] R. H. Koch *et al.*, Phys. Rev. Lett. **63**, 511 (1989); P. L. Gammel, L. F. Schneemeyer, and D. Bishop, Phys. Rev. Lett. **66**, 953 (1991).

[17] N. Motohira, K. Kuwahara, T. Hasegawa, K. Kishio, and K. Kitazawa, J. Ceram. Soc. Jpn. Int. Ed. **97**, 994 (1989).

[18] T. W. Li, P. H. Kes, N. T. Hien, J. J. M. Franse, and A. A. Menovsky, J. Crys. Grow. **135**, 481 (1993).

[19] T. W. Li *et al.*, Physica C **224**, 110 (1994).

[20] H. Vichery *et al.*, Physica C **159**, 697 (1989); A. Legris *et al.*, J. Phys. I **3**, 1605 (1993); F. Rullier-Albenque, A. Legris, H. Berger, and L. Forro, Physica C **254**, 88 (1995).

[21] V. Hardy *et al.*, Nucl. Instr. Meth. B **54**, 472 (1991).

[22] E. Zeldov *et al.*, Phys. Rev. Lett. **73**, 1428, (1994); D. Majer *et al.*, in "Coherence in High-Temperature Superconductors" edited by G. Deutscher and A. Revcolevschi, World Scientific (Singapore), 271 (1996).

[23] G. Yang *et al.*, Phys. Rev. B **48**, 4054 (1993); T. Tamegai *et al.*, Physica C **223**, 33 (1993); K. Kishio *et al.*, in "Proc. 7th Intnl. Workshop on Critical Currents in Superconductors" ed. H.W. Weber, World Sci. Pub., Singapore, p. 339 (1994).

[24] T. Hanaguri *et al.*, Physica C **256**, 111 (1995).

[25] Y. Yamaguchi *et al.*, Physica C **246**, 216 (1995).

[26] B. Revaz *et al.*, Europhys. Lett., **33**, 701 (1996).

[27] J. A. Fendrich *et al.*, Phys. Rev. Lett. **74**, 1210 (1995).

[28] Y. Imry and M. Wortis, Phys. Rev. B **19**, 3580 (1979).

[29] G. I. Menon and C. Dasgupta, Phys. Rev. Lett. **73**, 1023 (1994).

[30] A.I. Larkin and V. M. Vinokur, Phys. Rev. Lett. **75**, 4666 (1995).

[31] R. Ikeda, J. Phys. Soc. Jpn. **65**, 1170 (1996).

[32] M.J.P. Gingras and D. A. Huse, Phys. Rev. B **53**, 15193 (1996); D. Ertas and D. R. Nelson (preprint); S. Ryu, A. Kapitulnik, and S. Doniach (preprint).

[33] E. Zeldov *et al.*, Europhys. Lett. **30**, 367 (1995).

[34] N. Chikumoto *et al.*, Phys. Rev. Lett. **69**, 1260 (1992); Physica C **185-189**, 2201 (1993).

[35] N. Morozov, E. Zeldov, D. Majer, and M. Konczykowski, Phys. Rev. B **54**, 3784 (1996).